Journal of JSEM, Vol. 8, Special Issue (2008) 88-93

Extraction of Singularities in Isoclinic Phase Map for Isoclinic Phase Unwrapping in Digital Photoelasticity

Pichet PINIT[1] and Eisaku UMEZAKI[2]

[1] King Mongkut's University of Technology Thonburi, 126 Prachautid, Bangmod, Thungkru, Bangkok 10140, Thailand
[2] Nippon Institute of Technology, 4-1 Gakuendai, Miyashiro, Saitama 345-8501, Japan

Abstract
The extraction of the singularities in the wrapped map of the isoclinic parameter photoelasticitally obtained is presented. The method involves the use of two wrapped maps of isoclinics and a map of modulated intensity. Two characteristics–the abrupt phase jumps around the singularities and the values of modulated intensity–are used to identify those positions. The technique developed herein is evaluated with the real phase maps of an eccentrically loaded split ring (C-shaped model) under compression and experimental results are also presented.

Key words
Digital Photoelasticity, Isoclinic Parameter, Phase Unwrapping, Singularities

1. Introduction

Based on phase-shifting technique (PST), two important problems affect the computation of isoclinic parameter, ϕ, i.e., the isochromatic-isoclinic interaction [1] and the wrapped phase of isoclinics. Recently, the present authors have proposed technique for solving the problems [2]. The technique does success to unwrap the wrapped phase of isoclinics by taking the existence of the singularities–isotropic and singular points–into the consideration.

The crucial step in that work is to detect the isotropic and singular points and only one wrapped isoclinic map was used. The binary-masked image representing the points detected showed some erroneous positions. It has been shown that these erroneous positions are unaffected on the phase unwrapping [2] if they are well controlled. However, these erroneous positions may delay the whole unwrapping process because they are kept to be lastly processed. That they are to be lastly treated makes unwrapping routine taking more time than that of their detection routine. This is due to the fact that the detection routine works quite faster than the unwrapping.Note that, the phase unwrapping algorithm proposed in Ref. [2] composes of the detection and unwrapping routines. Therefore, if they are correctly detected from the start, this may speed up the unwrapping routine (also the whole process).

Moreover, in the view of engineering (optimum) design, the correct positions of the isotropic and singular points are necessary. This is because at these points, stresses are equal to zero. Then, holes used for passing electrical wires, for example, in the structural members should be drilled at these points. This also reduces the weight of the members designed without any change of their external shapes [4] and, furthermore, the stress field remains nearly unaltered under loads.

For just mentioned reasons, in this paper, the detection of isotropic and singular points based on the combination of the wrapped maps of isoclinics is presented. The load application points or supports which behave as if they were singularities are taken into the consideration. Further, the use of the map of modulated intensity which directly relates to the magnitude of the principal-stress difference, $(\sigma_1 - \sigma_2)$, for helping the detection routine is addressed. The detection technique is evaluated by applying to the eccentrically loaded split ring (C-shaped model) under compression.

2. Numerical Computation of Isoclinic Parameter

An intensity equation for the dark-field setup of the plane polariscope with a white light source for an arbitrary phase shifted angle position m can be expressed as [1]

$$I_{m,\lambda} = \frac{1}{\Delta\lambda}\int_{\lambda_{\text{lower}}}^{\lambda_{\text{upper}}} I_{\text{p},\lambda}\sin^2(\pi N_\lambda)\sin^2 2(\phi-\theta_m)d\lambda + I_{\text{b},\lambda} \tag{1}$$

where $\Delta\lambda = \lambda_{\text{upper}}-\lambda_{\text{lower}}$, λ_{upper} and λ_{lower} are the upper and lower limits of the spectrum of the light source, $I_{\text{p},\lambda}$ is the intensity of the polarized light coming out of the polarizer, N_λ is the relative or fractional fringe order for a given primary wavelength λ (= R, G, B) of the white light source, ϕ is the isoclinic parameter or the angle between σ_1 direction and the reference axis (horizontal axis), θ is the induced phase-shifted angle and $I_{\text{b},\lambda}$ is the total background intensity.

The relative fringe order relates to the relative retardation and $(\sigma_1 - \sigma_2)$ in plane-stress state by

$$\frac{\delta_\lambda}{2\pi} = N_\lambda = \frac{C_\lambda h}{\lambda}(\sigma_1-\sigma_2) = \frac{h}{f_{\sigma,\lambda}}(\sigma_1-\sigma_2) \tag{2}$$

where δ_λ is the relative retardation, C_λ is the stress-optic coefficient, $f_{\sigma,\lambda}$ is the material stress fringe value for which its value can be obtained by calibration method and h is the thickness of the tested model.

Applying the four-step phase shifting method to the intensity equation of the dark-field configuration of the plane polariscope using the white light as a light source, yields the equation for determining the isoclinic parameter as [2, 3]

$$\phi_{\mathrm{w}} = \frac{\pi}{8} - \frac{1}{4}\arctan\left(\frac{I_1^{\mathrm{s}} - I_3^{\mathrm{s}}}{I_2^{\mathrm{s}} - I_4^{\mathrm{s}}}\right) \quad \text{for } I_{\mathrm{mod}}^{\mathrm{s}} \neq 0 \tag{3}$$

where

$$I_{\mathrm{m}}^{\mathrm{s}} = \sum_{\lambda} I_{m,\lambda} \tag{4}$$

$$I_{\mathrm{mod}}^{\mathrm{s}} = \sqrt{\left(I_1^{\mathrm{s}} - I_3^{\mathrm{s}}\right)^2 + \left(I_2^{\mathrm{s}} - I_4^{\mathrm{s}}\right)^2} \tag{5}$$

Equation (3) gives $\phi_{\mathrm{w}} \in [0, +\pi/4]$ due to the use of the ordinary arctangent function and the subscript 'w' denotes the wrapped value. Note that $[0, +\pi/4]$ means $0 \le \phi_{\mathrm{w}} \le +\pi/4$ whereas $(-\pi/4, +\pi/4]$ means $-\pi/4 < \phi_{\mathrm{w}} \le +\pi/4$ and this identity can be applied to other ranges.

3. Definition of Singularities

Singularities are the properties of some points in the loaded structural member at which the state of stress satisfies certain specified conditions. Based on the state of stress in a plane problem, there are two singularities occurring in the map of isoclinics, i.e., an isotropic point and a singular point.

Apart from these two singularities, in Ref. [2], the load application points or supports were also treated as if they were singular point (actually they are not) because the variation of isoclinics around them unreliable, in which case unreliable isoclinics can cause failure in the phase unwrapping. Further, it is by nature that isoclinic of some parameters pass through the load application points or supports; therefore, these points are also treated as one of singularities (singular point).

3.1 Isotropic point

The isotropic point is a point at which the state of stress is hydrostatic, i.e., $\sigma_1 = \sigma_2 = \sigma \neq 0$ (or = 0) [6]. At this point, isoclinics of all different parameters of ϕ can pass through and intersect each other. Since the physical range of isoclinics is of $(-\pi/2, +\pi/2]$ with modulo $+\pi$ operation, in the isoclinic maps of the ranges of $[0, +\pi/2]$ and $(-\pi/4, +\pi/4]$, there exist lines representing the abrupt jumps of isoclinics passing through the isotropic point.

These abrupt phase jumps have the same sign and this sign identifies the type of the isotropic point, i.e., positive or negative type. If an isotropic point is of positive type, the isoclinics gradually vary around such point counterclockwise. On the other hand, that point is of negative type if the isoclinics vary clockwise around it.

Generally, an isotropic point represents itself as a point but in an experiment, it may present as a small region. Further, for some models, it may appear as a line. Recall the neutral axis of the beam under pure bending.

3.2 Singular point

A singular point is a special case of an isotropic point; that is, it is a point at which the state of stress satisfies the condition $\sigma_1 = \sigma_2 = 0$. At this point, isoclinics of some parameters of ϕ can pass but they do not intersect each other because they converge at a singular point. The reason is that a singular point is always on free boundaries at which the shear stress is equal to zero (shear-free boundaries).

The number of the lines representing the abrupt phase jumps converging at a singular point is difficult to predict because the position on the model boundaries at which the isoclinics converges depends on the geometrical shape of the model and/or load condition. This is evident that, for some models (e.g., circular disk under compression), the points along their free boundaries appear to be a series of singular points and in this case they form a singular line [5] whereas a singular point obviously appears as a point on the boundaries of the circular ring under compression [6].

A singular point usually represents a change in sign of stress, i.e., a transition from tension to compression [6]. Further, from the observation of the wrapped maps of isoclinics, it reveals that the sign of a singular point is of negative type [2, 7, 8].

3.3 Load application point and support (Poles)

Load application points are points at which an action load exerts on the structure whereas supports are those at which a reaction load occurs. For simplicity, they are termed as a pole [4].

The state of stress at a pole becomes $(\sigma_1 - \sigma_2) \to \infty$ and this is because the fringe density at and near a pole is very high due to the applied loads. The number of the lines converging at a pole is also difficult to predict as in the case of a singular point; however, a pole is of positive type [2, 7, 8].

3.4 Modulated intensity

As seen in Eq. (1), the modulated intensity can be defined as the following term.

$$I_{m,\lambda} = \frac{1}{\Delta\lambda}\int_{\lambda_{\mathrm{lower}}}^{\lambda_{\mathrm{upper}}} I_{\mathrm{p},\lambda} \sin^2(\pi N_{\lambda}) d\lambda \tag{6}$$

It is seen that $I_{\mathrm{mod},\lambda}$ is a function of fringe order which relates to the principal-stress difference by Equation (2). Since at an isotropic point or singular point $(\sigma_1 - \sigma_2) = 0$, at that point $N_{\lambda} = 0$. Then, an isotropic point can be clearly seen in the raw fringe patterns of the model when it is under the field of white light in the circular polariscope.

Since the modulated intensity is numerically obtained from those fringe patterns (Eq. (5)), it can help in the detection routine.

4. Method of Detection

The method of detection of singularities is as following.

- Border isolation: this stage isolates points or regions around the boundaries of the model. The main purpose of this stage is to detain the unreliable isoclinics such that they are lastly

processed by the phase unwrapping routine. Since a singular point and pole are on the boundaries, they are also isolated. However, this stage is optional; that is, a user can choose to isolate only singular points and poles.

- Detection of isotropic point: this is done by performing a raster scan over the isoclinic maps of the ranges of [0, +π/2] and (−π/4, +π/4] and the map of modulated intensity using technique in Ref. [2]. Note that at this stage all detected points are tentative isotropic point and they are separately registered into three binary arrays which will be described next.

- Selection of singularities: since in all three arrays, the pixels representing the positions of singularities are set as 0-valued pixel. Then, any pixel is a isotropic point, singular point or pole if such pixel has 0-valued for all three arrays.

5. Experimental Results and Discussion

The system used for recording the photoelastic fringe images is a plane polariscope with the white light source (halogen lamp). A digital camera model SLR D70 of Nikon was used to capture the photoelastic fringe images. The geometrical dimension of the C-shaped model and the direction of the applied load and support are shown in Fig. 1. The model was made of an epoxy resin plate.

When performing the experiment, it was vertically subjected to the eccentrically compressive load P = 157 N. The raw color fringe images of the model digitally collected according to the four different orientations of the dark-field configuration of the plane polariscope are reported in Fig. 2.

5.1 Maps of wrapped isoclinics

Applying Eq. (3) to those images shown in Figs. 2(a)-(d) yields the map of wrapped isoclinics of the range of [0, +π/4] (Fig. 3(a)). The maps of wrapped isoclinics of the ranges of [0, +π/2] and (−π/4, +π/4] obtained from Fig. 3(a) using the simple logic operations [2] are shown in Figs. 3(b) and (c), respectively, whereas Fig. 3(d) reports the map of modulated intensity obtained using Eq. (5).

It is clearly seen that all isoclinics pass through the isotropic point (Figs. 3a-c). Nevertheless, the position of the isotropic point is not so clear and it appears to be a region and can be confirmed by comparing Fig. 3d with that reported in Ref. [6] (see block in Fig. 3d).

Apart from such region, there are two more isotropic points (inside circle marks); however, these are not the isotropic point but, in fact, they are singular point and they should be exactly on the sharp edges. That they appeared as if they were an isotropic point is due to the fact that the residual stress or edge stress occurring when the model being prepared might force them to move toward inside. They also can be observed in all wrapped maps of isoclinics (Figs. 3(a)-(c)).

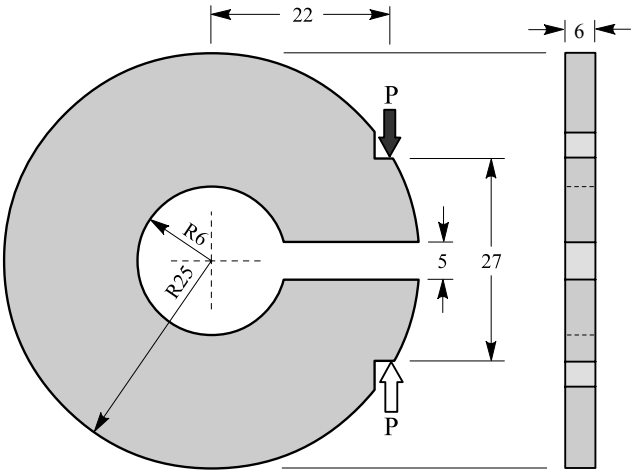

Fig. 1 Applied load direction and dimensions of the split ring under eccentrically compressive load P of 157 N. The black and white arrows indicate the applied load direction and the reaction at the supports, respectively. (Geometrical unit: mm and image not to scale)

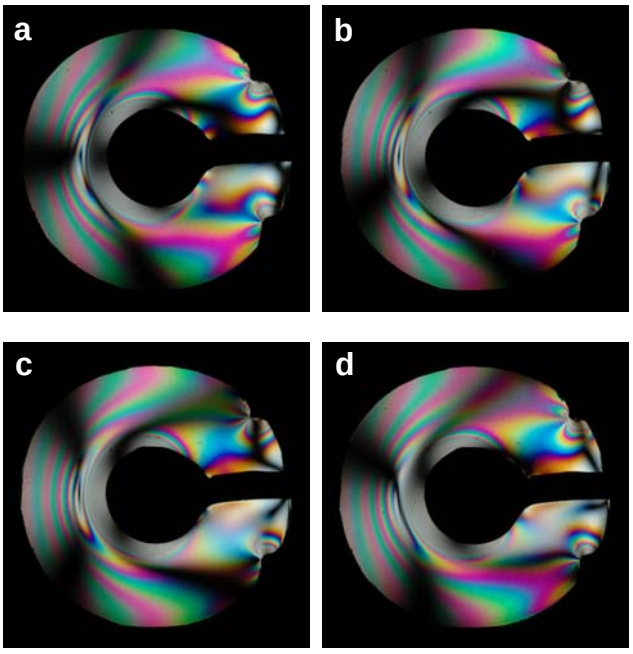

Fig. 2 Raw color photoelastic fringe images of the model with different setup of the polariscope system: (a) θ_1= 0, (b) θ_2 = +π/8, (c) θ_3 = +π/4, and (d) θ_4 = +3π/8. The size of the images is 512 × 512 pixels.

5.2 Representation of detected singularities

Binary image shown in Fig. 4a was given by performing a raster scan over the map of wrapped isoclinics of the range of [0, +π/2] (Fig. 3b). On similar line, Figs. 4(b) and (c) were given from Figs. 3(c) and d. The size of window used for such scanning was 31 × 31 pixels and the threshold used for identifying abrupt jumps of isoclinics around the isotropic region was set to be +0.3π/2. In this case, +π/2 is

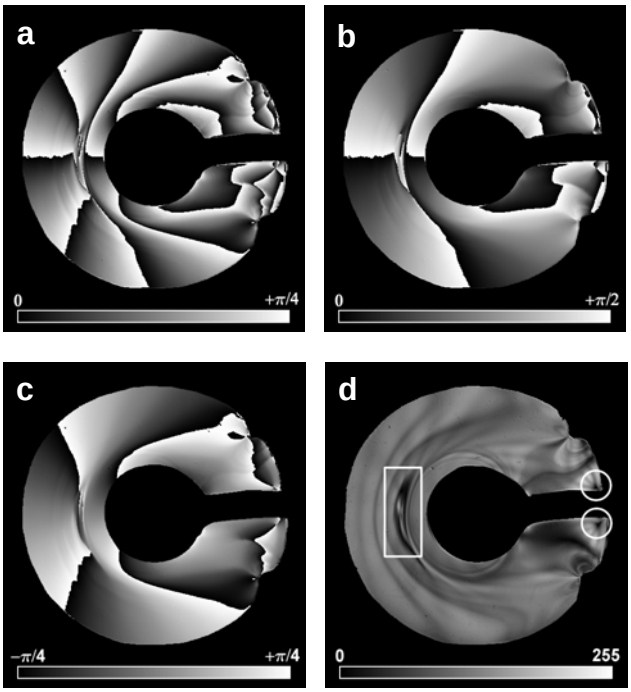

Fig. 3 Maps of wrapped isoclinics with different ranges and map of modulated intensity: (a) [0, +π/4], (b) [0, +π/2], (c) (−π/4, +π/4], and (d) normalized map of modulated intensity. Note that the actual values of modulated intensity are in the range [0, 1].

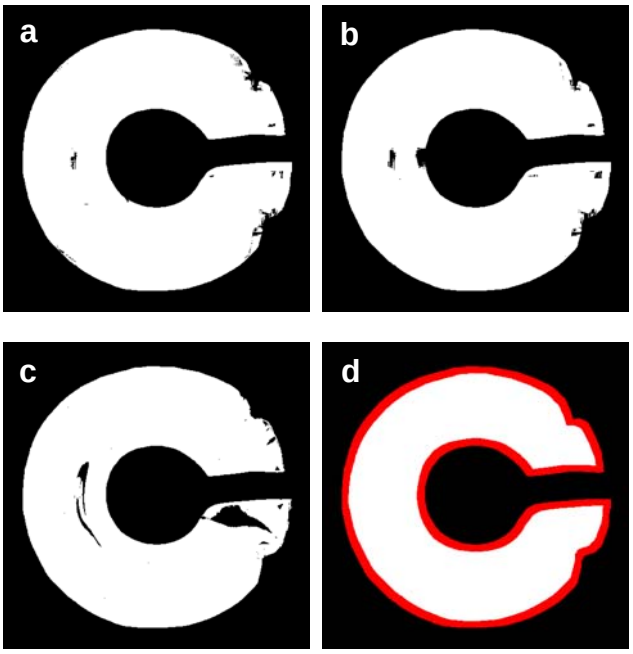

Fig. 4 Binary images representing the position of singularities: (a) image given from scanning over Fig. 3b, (b) image given from scanning over Fig. 3(c), (c) image given from scanning over Fig. 3(d) and (d) isolated region (red region).

the modulo of the ranges of [0, +π/2] and (−π/4, +π/4]. It is worthy to note that the default value of the threshold is +0.8π/2 [2]. The value of +0.3π/2 was used because it was difficult to identify the abrupt jumps around the isotropic region as it is rather vague. Further, Fig. 4(c) was obtained from the condition that if a value of modulated intensity (Eq. (5)) for every point was less than or equal to 15% of their maximum value, such point was treated as one of singularities.

Observing Figs. 4(a)-(c) reveals that the large black region appearing on the right side of the isotropic region in Fig. 4(c) is not the real one. This can be confirmed by closely considering Fig. 2. At that region, there is no black color which represents the isotropic region. However, it did happen because of the effect of the background intensity. As seen in the map of modulated intensity, such region appears dark (Fig. 3(d)) and this affects the computation of isoclinics; that is, Eq. (2) is unreliable when the fringe order is equal or close to zero or integer number. The result of this effect is clearly seen on the map of the range of (−π/4, +π/4] where the ragged line appears (see the line representing the abrupt jumps of isoclinic). In Figs. 4(a) and (b), there are several black regions around the load application point and support. These regions are the pole.

By using Figs. 4(a)-(c), the binary image obtained is shown in Fig. 5(a) (see black line inside red circle mark). This was done by performing a raster scan over them and checking the binary triplet; that is, for the point or pixel at the same position in these three images (three binary arrays) was preserved as an isotropic point if its binary triplet value was (0,0,0). For other conditions, e.g., (0,0,1), (1,1,0), ..., that pixel was finally set as 1-valued pixel. It is seen that the isotropic points were found as a thin line. Figure 5(b) shows the expanded version of such line for the purpose of clarity. The circle window with radius of 15 pixels was used to implement this.

Since all singularities affect the performance of the phase unwrapping algorithm [2], they must be kept for last processing. Then, those regions representing the singular point and poles can be easily masked out by scanning along boundary of the binary image. With the window size of 13 × 13 pixels, the singular point and pole (also other unreliable pixels) were isolated as shown in Fig. 4(d) (red region). Note that, actually, in the binary array the red region is black (0-valued pixels); however, it is shown as red color for the sake of clarity. It should be noted here that, as the first attempt, the window size used for detection of singularities was of 21 × 21 pixels and the threshold used for identifying abrupt jumps of isoclinics was of +0.8π/2. This was done because of the fact that the smaller the size of the detecting window is, the fewer the scanning process takes time. The positions of singularities found were almost the same as those reported in Figs. 4(a)-(c) with smaller regions. After performing a raster scan for the binary triplet, the obtained binary image contained no singularities. However, for the binary doublet (Figs. 4(a) and (b)), the isotropic region was detected.

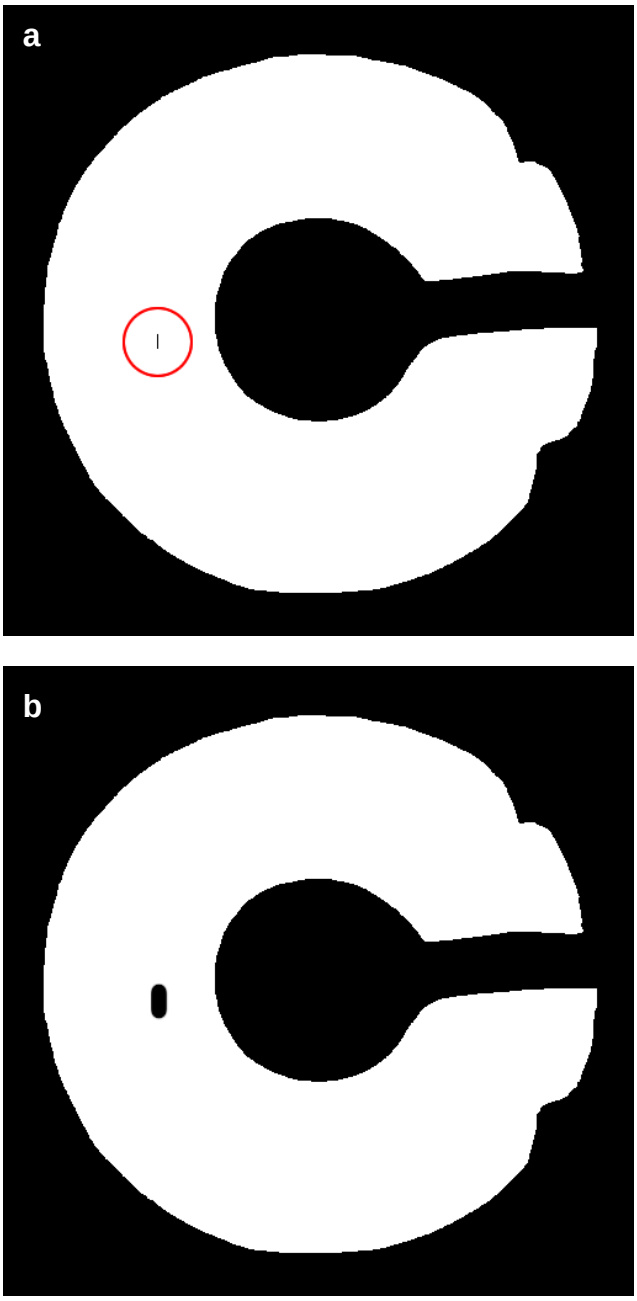

Fig. 5 Binary images representing position of the isotropic region: (a) binary image obtained by checking binary triplet and (b) binary image obtained by expanding the isotropic region in (a).

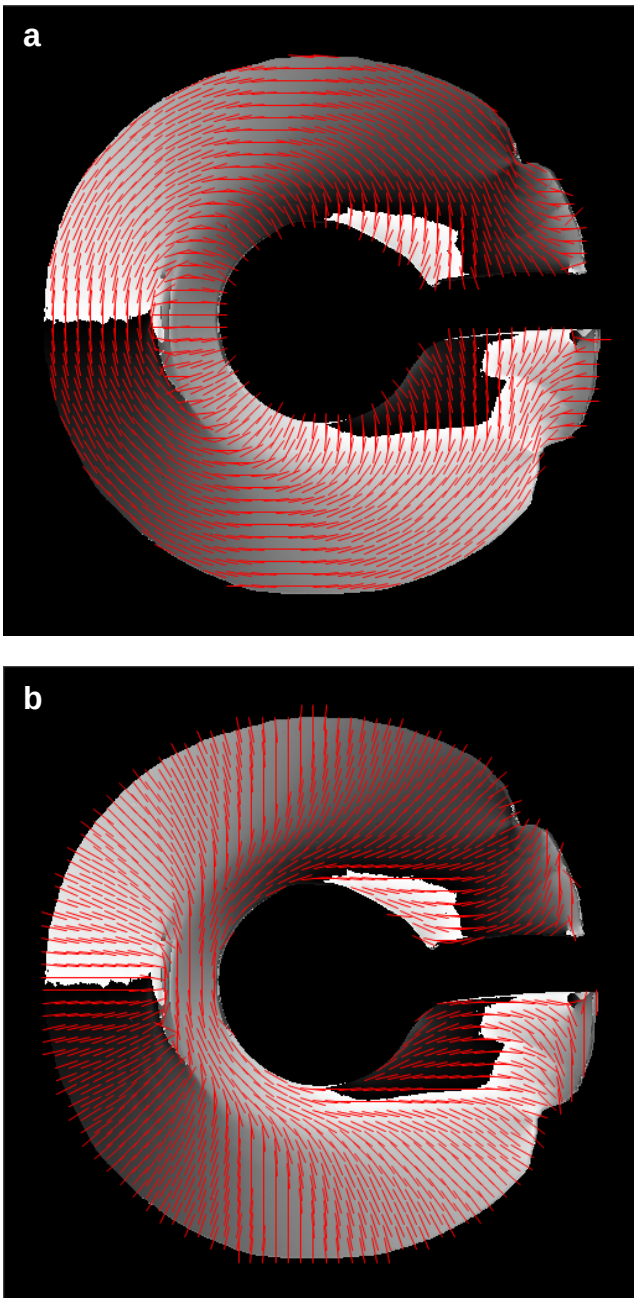

Fig. 6 Stress trajectories or isostatics of σ_1 and σ_2 drawn over the map of unwrapped isoclinics: (a) σ_1 isostatics and (b) σ_2 isostatics.

Considering Figs. 4(a) and (b) reveals that the isotropic region found should be larger than they were because the size of window used to detect them is quite large. This is because of the unsmooth isoclinics with small abrupt jumps around the isotropic region. However, the appearance of the unsmooth isoclinics with small abrupt jumps may come from the fact that the model is not perfectly fabricated and the directions of the applied load are not exactly vertical.

Figure 6 shows the stress trajectories plotted over the unwrapped map of isoclinics. Since, in general, $\sigma_1 \geq \sigma_2$, the major part of the outer boundary of the model between the applied loads is all under tension and this can be observed the σ_1 isostatics (Fig. 6(a)). Further, it is seen that the trajectories are parallel to the outer boundary up to the points of applied loads and then they turn and become normal to the boundary [6].

Similarly, the major part of the inner boundary of the model is all subjected to the compression (Fig. 6(b)). This can be verified by considering the inner boundary of the

model shown in Fig. 6(b). If the σ_1 and σ_2 stress trajectories are combined together, one could see that they form the interlocking trajectories around the isotropic point shown in Fig. 5. This means that the isotropic region is of positive type; that is, the isoclinic values gradually vary from $-\pi/2$ (black) to $+\pi/2$ (white) counterclockwise around the isotropic region.

Although the technique works under just mentioned circumstances, which are the typical problem in the real world, the results reveal that the isotropic region is still found and this may be considered as the good point of the technique proposed herein. However, for better results, caution must be paid when performing the experiment.

6. Conclusion

In this paper, the technique for detection of singularities has been proposed. The technique is based on the use of the two wrapped maps of isoclinics in the ranges of $[0, +\pi/2]$ and $(-\pi/4, +\pi/4]$, the map of modulated intensity.

Results of the binary images show that the isotropic point or region can be found using the binary triplet and further, singular point and poles are detected and isolated. This eases the phase unwrapping algorithm already proposed in Ref. [2] and help in the optimum design [4]. Further, although three binary arrays are used here whereas two arrays (Figs. 4(a) and (c)) were used in Ref. [2], the time used to perform scanning is not much different because the operation works on the binary image. For the whole process, the time taken by the phase unwrapping algorithm coupled with the technique proposed here is fewer than that reported in Ref. [2] when the size of the fringe image becomes large.

As seen in Fig. 4(c) that the isotropic regions found are nearly close to those shown in Figs. 3(a) and (b); however, some points inside such regions were discarded by the triplet regulation. Therefore, before performing to find the binary triplet value, it might be better to expand such regions. Further, for the expanded regions, if there are many of them and they are close enough within a specific length, joining them might give better results.

The model studied here posses the isotropic region which presents a certain level of difficulties. However, for other models having the isotropic point, it is thought that the technique would give good results. This may improve the performance of the phase unwrapping algorithm and also help in design as previously mentioned.

References

[1] Ramesh, K.: Digital Photoelasticity: advanced techniques and applications, Springer, Berlin, (2000), 157, 231.

[2] Pinit, P. and Umezaki, E.: Digitally Whole-field Analysis of Isoclinic Parameter in Photoelasticity by Four-step Color Phase-shifting Technique, *Opt. Lasers Eng.*, **45** (2007), 795-807.

[3] Pinit, P. and Umezaki, E.: Full-field determination of principal-stress directions using photoelasticity with plane polarized RGB lights, *Opt. Rev.*, **12** (2005), 228-232.

[4] Umezaki, E. and Shimamoto, A.: Application of Isotropic Points Extracted Using Computerized Photoelastic Experiment to Design Structural Members, *J. Strain Ana.*, **35** (2000), 415-421.

[5] Jessop, HT. and Harris, FC.: Photoelasticity: principles and methods, Dover, New York (1950), 74-77.

[6] Frocht, M.M.: Photoelasticity, Vol. 1, John Willey & Sons, New York (1941), 189-191, 209-213.

[7] Pinit, P. and Umezaki, E.: Isoclinic Evaluation of Circular Disk under Three Radial Loads and Angular Plate Models by Four–Step Color Phase Shifting Technique, *Proc. 2006 Int. Symp. on Advanced Fluid/Solid and Technology in Experimental Mechanics*, Sapporo, (2006), 45-50.

[8] Pinit, P. and Umezaki, E.: An Automated Phase Unwrapping Algorithm for Isoclinic Parameter in Phase-Shifting Photoelasticity, *Proc. the 13rd Int. Conf. on Experimental Mechanics*, Alexandroupolis, (2007), on CD-ROM.